http://dx.doi.org/10.5012/bkcs.2011.32.10.3793

Morphological Evolution of Ag_2O Microstructures from Cubes to Octapods and Their Antibacterial Activities

Myeong-Jin Kim, Sunghyen Kim,† Heonyong Park,† and Young-Duk Huh*

*Department of Chemistry and †Department of Molecular Biology, Institute of Nanosensor and Biotechnology, Dankook University, Gyeonggi-Do 448-701, Korea. *E-mail: ydhuh@dankook.ac.kr*
Received August 4, 2011, Accepted August 18, 2011

Key Words : Morphology evolution, Crystal growth, Silver oxide, Antibacterial activity

The selective synthesis of inorganic oxides with unique morphology has attracted considerable interest because of their morphology-dependent properties and applications.[1-3] Efforts on most synthetic inorganic oxides have been focused on preparing a stable morphology rather than providing a strategy for producing various morphologies. Therefore, well-controlled methods for synthesizing inorganic oxides with a systematic evolution of morphology should be developed by adjusting the experimental conditions. Among the morphology-controlled syntheses of inorganic oxides, cuprous oxide (Cu_2O) has been widely investigated due to its ease of preparation.[4-8] The morphology-dependent photocatalytic and antibacterial properties of Cu_2O were also studied recently.[9-11] Although Cu_2O and silver oxide (Ag_2O) have similar cubic crystal structures, relatively little is known about the morphology-controlled synthesis and physical properties of Ag_2O.[12,13] To date, a study of the morphology-dependent antibacterial effect of Ag_2O has reported only for different polyhedral shapes including octahedrons, truncated octahedrons, and cubes.[14] This study provided a simple precipitation method for the morphological evolution of Ag_2O from cubes to octapods. Furthermore, the morphology-dependent antibacterial activity of Ag_2O against *E. coli* was also examined.

Ag_2O products with various morphologies were prepared from a silver-pyridine (Py) complex solution. Pyridine was used as the ligand for the Ag^+ ions. Pyridine combined with the Ag^+ ions to form a $[Ag(Py)_2]^+$ complex. This complex reacted with OH^- by adding NaOH, which was then dehydrated to produce Ag_2O. The chemical reactions producing Ag_2O are as follows:

$$2\,Ag^+(aq) + 4\,Py \rightarrow 2\,[Ag(Py)_2]^+(aq) \quad (1)$$

$$2\,[Ag(Py)_2]^+(aq) + 2OH^-(aq) \rightarrow Ag_2O(s) + 4\,Py + H_2O \quad (2)$$

Figure 1 shows the X-ray diffraction (XRD) patterns of Ag_2O prepared using different amounts of $AgNO_3$ with 1.0/40/10 molar ratios of $AgNO_3$/pyridine/NaOH, respectively. All peaks corresponded to those reported for bulk Ag_2O (JCPDS 12-0793, a = 0.4736 nm) with a cubic structure and impurities. Figure 2 shows scanning electron microscopy (SEM) images of Ag_2O prepared with different amounts of $AgNO_3$. At 2.5 mL of $AgNO_3$, Ag_2O formed a regular cubic shape, as shown in Figure 2(a). The mean length of each side was 600 nm. At 5.0 mL of $AgNO_3$, Ag_2O formed a cubic shape, and the mean length of each side was 700 nm. Void spaces were created at the center of the cubic crystal planes, as shown in Figure 2(b). When the amount of $AgNO_3$ was increased to 7.5 mL, the void spaces at the center of the cubic crystal planes increased further, as shown in Figure 2(c). As the amount of $AgNO_3$ was increased up to 20 mL, octapods with eight identical Ag_2O horns were formed (Figure 2(d)).

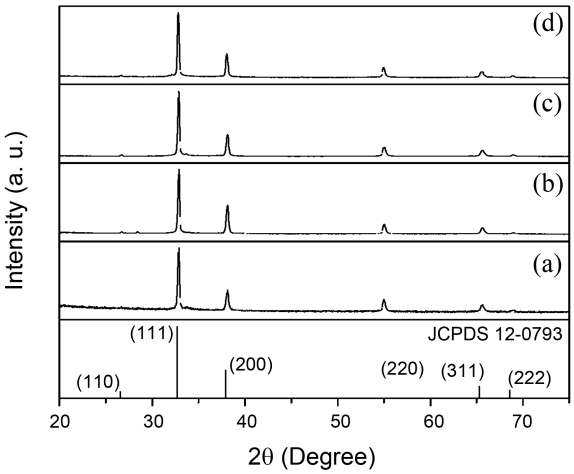

Figure 1. X-ray diffraction patterns of Ag_2O prepared with different amounts of $AgNO_3$; (a) 2.5 mL, (b) 5.0 mL, (c) 7.5 mL, and (d) 20 mL.

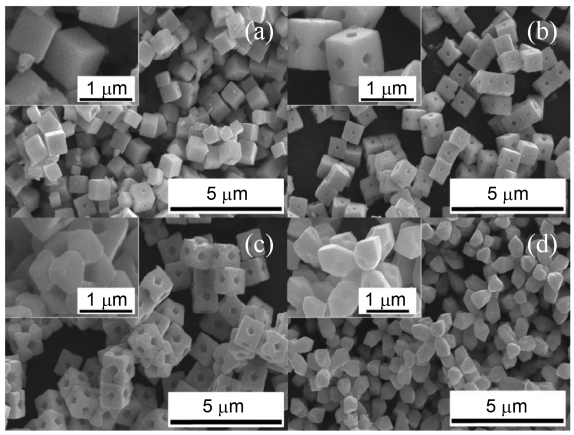

Figure 2. SEM images of Ag_2O prepared with different amounts of $AgNO_3$; (a) 2.5 mL, (b) 5.0 mL, (c) 7.5 mL, and (d) 20 mL.

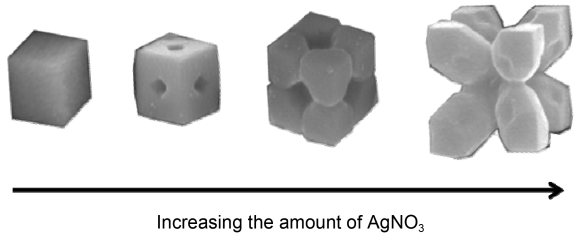

Figure 3. Schematic morphology of Ag_2O microcrystal evolution from cubes to octapods with increasing amounts of $AgNO_3$.

Generally, morphology of a crystal is affected by both kinetic and thermodynamic growth processes.[15,16] Crystals with simple shapes, such as spheres, cubes and octahedrons, are formed to minimize the total surface free energy in thermodynamic equilibrium. However, crystals with branched shapes, such as hexapods and octapods, are formed by kinetic growth processes. The reaction rate for forming Ag_2O is very slow at 2.5 mL of $AgNO_3$. Therefore, a thermodynamically controlled reaction occurred, and cubic Ag_2O was formed with the smallest amounts of $AgNO_3$. As the amount of $AgNO_3$ increased, the reaction rate of Ag_2O formation increased. Larger void spaces were formed at the cubic crystal planes by increasing the reaction rate. Finally, a large increase in reaction rate with a large amount of $AgNO_3$ improved the degree of branching, and the Ag_2O morphology finally evolved into an octapod. Therefore, the various morphologies of Ag_2O microcrystals in this work were formed by a kinetically-controlled process with increasing amounts of $AgNO_3$. Figure 3 shows a schematic diagram of the morphological evolution of Ag_2O microcrystals with an increasing amount of $AgNO_3$.

Figure 4 shows *E. coli* grow rates in the absence or presence of various Ag_2O morphologies. Figure 4 clearly shows that all Ag_2O microcrystals caused an *E. coli* growth delay. The incubation times to grow up to 50% (half-maximal growth times) were 5.0, 9.9, 10.3, 11.0, and 12.0 h in the absence and presence of cubic, cubic with small voids, cubic with large voids, and octapods of Ag_2O, respectively. Moreover, bacterial growth was dependent on Ag_2O morphology. The antibacterial activities of Ag_2O prepared in this work were in the following order: cubes > cubes with small voids > cubes with large voids > octapods. This result suggests that the morphology of Ag_2O particles affects antibacterial activity. Cubic Ag_2O crystals are enclosed by (100) planes. The surfaces of the (100) planes are polar due to alternating layers of the Ag^+ cation and O^{2-} anions. Ag^+ ions are toxic and kill bacteria through a denaturation or oxidation mechanism.[14,17] Therefore, exposing cubic surface Ag^+ cations in Ag_2O crystals may enhance their antibacterial activity.

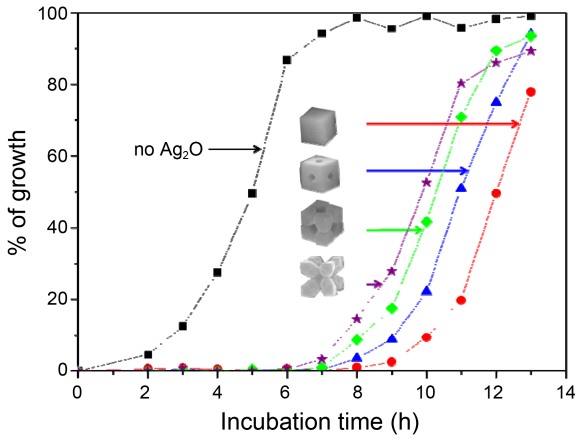

Figure 4. *E. coli* growth rates in the absence of Ag_2O (squares) and the presence of Ag_2O prepared with different amounts of $AgNO_3$; (a) 2.5 mL (circles), (b) 5.0 mL (triangles), (c) 7.5 mL (diamonds), and (d) 20 mL (stars).

Various Ag_2O microcrystal morphologies were prepared selectively using a silver-pyridine complex solution. By increasing the amount of $AgNO_3$, the morphology of the Ag_2O microcrystals evolved from simple cubes to octapods. Morphology-dependent antibacterial activity of Ag_2O against *E. coli* was observed. Exposure of Ag^+ cations from the (100) crystal planes of Ag_2O may play an important role in the antibacterial activity against *E. coli*.

Experimental Section

$AgNO_3$ (Aldrich, 99.0%), NaOH (Aldrich, 97%), pyridine (Aldrich, 99.8%), and dimethyl sulfoxide (DMSO, Aldrich, 99.9%) were used as received. In a typical synthesis of cubic Ag_2O, a mixed solution of water (994.2 mL), 0.1 M $AgNO_3$ aqueous solution (2.5 mL), and pyridine (0.848 mL) was prepared, and then a 1.0 M NaOH aqueous solution (2.5 mL) was quickly added to the mixed solution. The molar ratios of $AgNO_3$, pyridine, and NaOH were 1.0, 40, and 10, respectively. The final mixed solution was incubated for 4 h at room temperature. A mixed solution of water (953.22 mL), 0.1 M $AgNO_3$ aqueous solution (20 mL), and pyridine (6.78 mL) was used to prepare the Ag_2O octapods, and then a 1.0 M NaOH aqueous solution (20 mL) was quickly added with the same molar ratios of $AgNO_3$, pyridine, and NaOH as those used to prepare cubic Ag_2O. The amounts of $AgNO_3$, pyridine, and NaOH used were eight times those for the preparation of cubic Ag_2O to prepare the Ag_2O octapods. To investigate the morphological evolution of Ag_2O, different amounts of $AgNO_3$ (5.0 mL and 7.5 mL) were also used with the same molar ratios of $AgNO_3$, pyridine, and NaOH as those used to prepare the cubic Ag_2O. The products were collected following centrifugation at 4000 rpm for 5 min and were sonicated with water and ethanol several times and then dried for 24 h at room temperature. The structure and morphology of the Ag_2O products was characterized by powder XRD (PANalytical, X'pert-pro MPD) and SEM (Hitachi S-4300), respectively.

The antibacterial effects of Ag_2O on *E. coli* growth rates were also investigated. First, *E. coli* cells were grown to an absorbance of 0.40 at 600 nm. Subsequently, 50 μL of the *E. coli* culture was aliquotted evenly into 1.5 mL of Luria-Bertani (LB) media containing 2 μg/mL of the various forms of Ag_2O. The inoculated *E. coli* cells were grown further in a

37 °C shaking incubator for various incubation times. *E. coli* densities were determined by the optical density at 600 nm. Ag_2O crystals were dissolved in DMSO to prepare the stock cubic and octapod Ag_2O crystal solutions. The optical density was monitored using a UV-vis spectrophotometer (Beckman DU-7500).

Acknowledgments. This study was supported by a 2010 Dankook University project for funding RICT.

References

1. Burda, C.; Chen, X.; Narayanan, R.; El-Sayed, M. *Chem. Rev.* **2005**, *105*, 1025.
2. Xu, H.; Wang, W.; Zhu, W. *J. Phys. Chem. B* **2006**, *110*, 13829.
3. Hua, Q.; Shang, D.; Zhang, W.; Chen, K.; Chang, S.; Ma, Y.; Jiang, Z.; Yang, J.; Huang, W. *Langmuir* **2011**, *27*, 665.
4. Xu, J.; Xue, D. *Acta Mater.* **2007**, *55*, 2397.
5. Chang, Y.; Zeng, H. C. *Cryst. Growth Des.* **2004**, *4*, 273.
6. Zhao, X.; Bao, Z.; Sun, C.; Xue, D. *J. Cryst. Crowth* **2009**, *311*, 711.
7. Siegfried, M. J.; Choi, K. S. *J. Am. Chem. Soc.* **2006**, *128*, 10356.
8. Song, H. C.; Cho, Y. S.; Huh, Y. D. *Mater. Lett.* **2008**, *62*, 1734.
9. Zhang, Y.; Deng, B.; Zhang, T.; Gao, D.; Xu, A. W. *J. Phys. Chem. C* **2010**, *114*, 5073.
10. Kuo, C. H.; Huang, M. H. *J. Phys. Chem. C* **2008**, *112*, 18355.
11. Pang, H.; Gao, F.; Lu, Q. *Chem.Commun.* **2009**, 1076.
12. Lyu, L. M.; Wang, W. C.; Huang, M. H. *Chem. Eur. J.* **2010**, *16*, 14167.
13. Murray, B. J.; Li, Q.; Newberg, J. T.; Menke, E. J.; Hemminger, J. C.; Penner, R. M. *Nano Lett.* **2005**, *5*, 2319.
14. Wang, X.; Wu, H. F.; Kuang, Q.; Huang, R. B.; Xie, Z. X.; Zheng, L. S. *Langmuir* **2010**, *26*, 2774.
15. Quan, Z.; Li, C.; Zhang, X.; Yang, J.; Yang, P.; Zhang, C.; Lin, J. *Cryst. Growth Des.* **2008**, *8*, 2384.
16. Jun, Y. W.; Lee, J. H.; Choi, J. S.; Cheon, J. *J. Phys. Chem. B* **2005**, *109*, 14795.
17. Lok, C. M.; Ho, C. M.; Chen, R.; He, Q. Y.; Yu, W. Y.; Sun, H.; Tam, P. K. H.; Chiu, J. F.; Che, C. M. *J. Bio. Inorg. Chem.* **2007**, *12*, 527.